Research Reports Spontaneous simulation of land surface temperature in Tianjin city, China

Spontaneous simulation of land surface temperature in Tianjin city, China

Ruci WANG[a], Yuji MURAYAMA[b]

Abstract

Monitoring and simulating land surface temperature (LST) by using satellite images is an essential approach to understand land use/cover changes, especially in developing countries where the availability of ground truth and statistical data is limited. This study analyzed the relationship between LST and land use/cover types in Tianjin city from 2005 to 2015. Then, based on the LST distribution maps, we simulated LST in 2025 by employing a hybrid model of the artificial neural network and the cellular automata. The results show that the LST is gradually increasing from 2005 to 2025 with the changes in the land use/cover. This study provides significative information for sustainable development and environmental protection in the future.

Key words: land surface temperature, urbanization, simulation, Tianjin city

1. Introduction

With the rapid urbanization and industrialization, land use/cover has changed enormously (Hao *et al*., 2016; Subasinghe *et al*., 2016). At the same time, heat island effect has received much attention in the urban planning, because there is a direct correlation between LST and land use/cover distribution (Estoque and Murayama, 2017). Urban sprawl, environmental damage and cropland loss are widely recognized as influencing factors to enhance the heat island phenomena (Li *et al*., 2011; Xu *et al*., 2010). LST monitoring is a comprehensive expression of urbanization and environmental protection.

Commonly, urban expansion has been emerged at the cost of reducing cropland and green area. The green space in the metropolitan area is the most effective land use/cover type to avoid LST in a consistent exorbitant condition (Phan *et al*., 2018). Therefore, analyzing the relationship between LST and land use/cover distribution is essential to keep abreast of the urban living environment. Simulating LST by considering land use/cover distribution can also promote urban structure to stability. Stability is the sustainability of land use pattern and ecological process, which reflects the coordination of regional land use pattern and environmental conditions (Frihy, 2017). Many studies have examined the spatiotemporal distribution of LST in different years and simulated the LST under different scenarios. Zhang *et al*. (2017) simulated LST under the urban park green space scenario and the absence of that scenario in Haidian district by using a hybrid model composed of EnKF-3DVar and cellular automata model. This paper concluded that the allocation of the urban green space is significant in sustainable development (Zhang *et al*., 2017). Maduako *et al*. (2016) predicted LST dynamics in 2028 and 2042 in Ikom city by employing an artificial neural network (ANN) model, and the result shows that if nothing is done to decline surface temperature, LST will increase. Even if there are many studies on LST, LST simulation for the prediction is still only experimental (Madurako *et al*., 2016). "Add or remove" of modeling variables will affect simulation outcomes. Furthermore, the LST depends mainly on geographical location, the structure of land use/cover and government policies. Therefore, a case study on a regional scale can provide valuable information for urban planning and sustainable development.

This analysis focuses on exploring the relationship between LST and the distribution of land use/cover to retrieve the spatiotemporal patterns of LST and simulate LST under the spontaneous scenario to observe temperature variation in Tianjin city. The spontaneous scenario, assumes the development trend of the study area in near future without natural disasters, economic crisis, and policy reform. To reflect LST change in the study area, and to reduce the influence of original data, we standardized the range of LST into 0 to 1. This normalization significantly decreased the influence of uncertain factors of LST pattern.

2. Materials and methods

2.1. Study area

The study area, Tianjin city, is the largest city which covers an area of 11,860 km^2 in northern China (Fig. 1). Tianjin port, which locates in the Binhai new area, is the top-level port and ranks fifth in the world (Song and van Geenhuizen, 2014). Tianjin city recorded China's highest per-capita Gross Domestic Product (GDP) with USD

a Graduate School of Life and Environmental Sciences, University of Tsukuba, Japan
b Faculty of Life and Environmental Sciences, University of Tsukuba, Japan
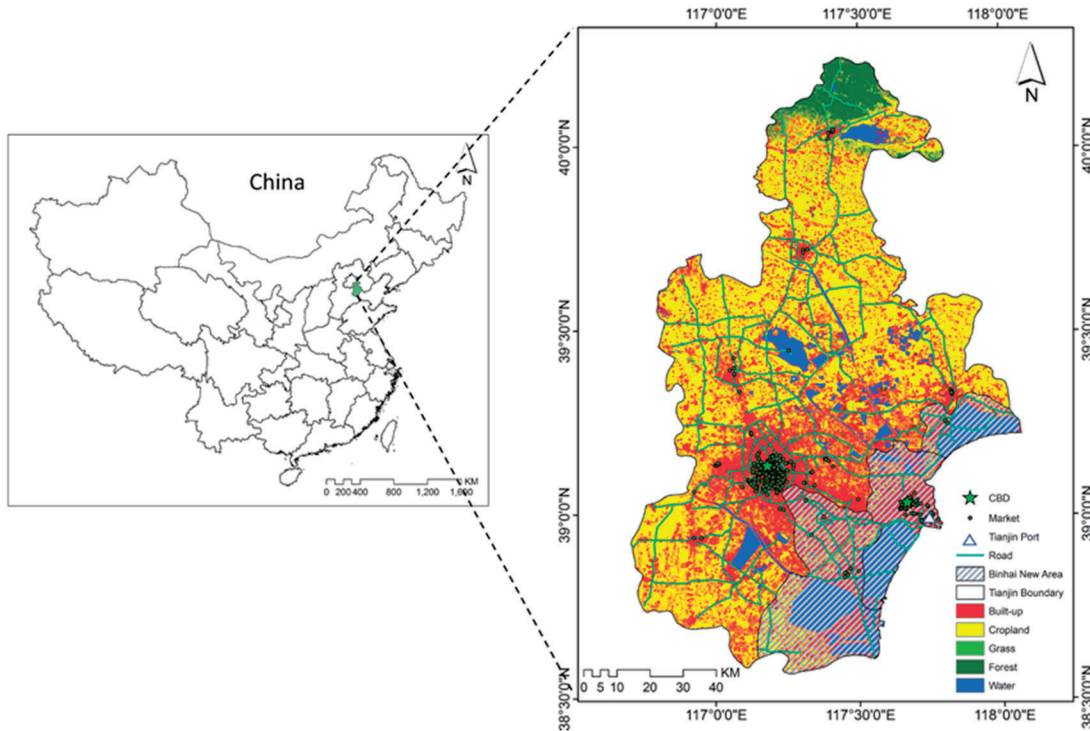
Fig. 1. Location of the study area.

17,126 in 2014. According to the National Bureau of Statistics (NBS) of China in 2015, 15.62 million people live in Tianjin in 2016, including 13.65 million people in the urbanized area ("National data," n.d.). The temperature in Tianjin city is distinctly different, season by season. The lowest monthly average temperature is -3.4 °C in January, and the highest is 26.8 °C in July.

2.2. Data used and pre-processing

Satellite images with high resolution, consistence and fast updating, have been selected to create LST maps for detecting the relationship between land use/cover and LST distribution. In this research, we selected eight images with cloud-free (less than 10%) in 2005 and 2015 from United States Geological Survey. All the Landsat images are in autumn and winter with 30-m spatial resolution. We also used the land use/cover maps in 2005 and 2015 which were collected from our previous research (Wang and Murayama, 2017). Other ancillary data, including Digital Elevation Model (DEM), slope, distance to built-up areas in 2015 and Normalized Difference Vegetation Index (NDVI) were also employed as modeling variables in the simulation.

To eliminate the effect of atmospheric and correct irradiation difference for different topography, TerrSet software has been employed for correction (Estoque and Murayama, 2017). After correction, the Digital Number

(DN) has been converted into surface reflectance values in multispectral bands, and at-satellite Brightness Temperature (TB) has been expressed in degrees Kelvin (Ranagalage et al., 2018).

2.3. Research flow

A framework is designed to simulate the LST map (Fig. 2). Three primary parts have been established. First, we used Landsat images to prepare NDVI and LST maps in Tianjin city. Second, using supervised maximum likelihood classification method, land use/cover maps were extracted. Third, we employed land use/cover map in each category as modeling variables into LST map and used ANN training to calculate transition trend. Next, by using a cellular automata model, the spatial distribution of LST map in 2015 was obtained. After that, we compared the simulated map with the actual LST map in 2015. If the result is within the tolerance, we continue to simulate LST map in 2025.

2.4. Calculation of the LST

Using Landsat thermal bands for calculating LST, the spectral emissivity (ε) is required. To retrieve the emissivity values, the thermal bands were used in the following equations (Weng et al., 2004):

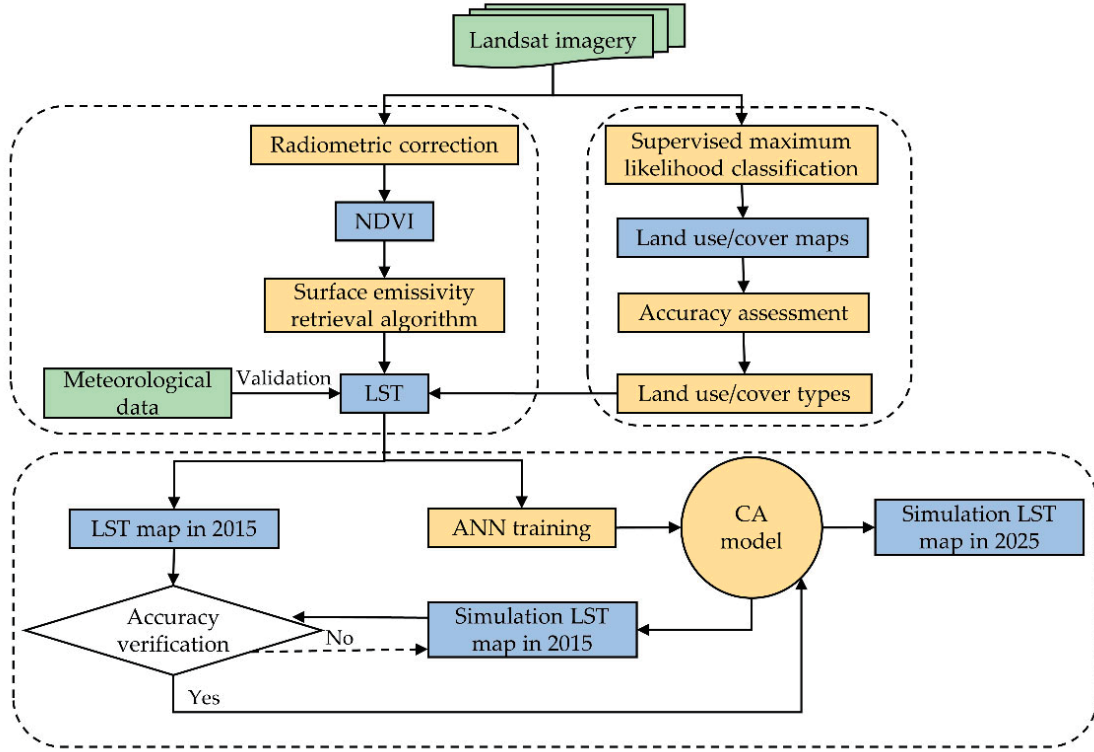$$LST = TB/[1 + (\lambda * TB/\rho) * \ln \varepsilon \qquad (1)$$

Fig. 2. Workflow of analyzing and simulating the LST distribution.

where TB = the Landsat TM band 6 or Landsat OLI/TIRS band 10 at-satellite brightness temperature in degrees Kelvin; λ = wavelength of emitted radiance (λ = 11.5 μm for Landsat TM band 5 and 10.8 μm for Landsat OLI/TIRS band 10); $\rho = h * \frac{c}{\sigma}$ (1.438 ∗ 10^{-2}mK), σ = Boltzmann constant (1.38 ∗ 10^{-23}J/K), h = Planck's constant (6.626 ∗ 10^{-34}Js), and c = velocity of light (2.998 ∗ 10^{8}m/s); ε = emissivity, and the equation can be expressed as:

$$\varepsilon = 0.004 * P_v + 0.986 \qquad (2)$$

where the proportion of vegetation (P_v) was expressed as follows:

$$P_v = \left(\frac{NDVI_{jr} - NDVI_{min}}{NDVI_{max} - NDVI_{min}} \right)^2 \qquad (3)$$

To calculate land surface emissivity values, NDVI method has been employed. The NDVI can be expressed as follows:

$$NDVI = (NIR\text{-}RED) / (NIR + RED) \qquad (4)$$

where NIR = the Landsat TM band 4 or Landsat OLI/TIRS band 5; RED = the Landsat TM band 3 and Landsat OLI/TIRS band 4.

Since the ranges of LST in different years are too diverse to compare, the normalization method has been applied to standardize the LST distribution maps (Li *et al*., 2013). In this study, LST results were normalized by using the fuzzy module in Terrset 18.31 software. The range of LST was normalized into 0 ~ 1.

2.5. Simulation procedure

There are many algorithms for the simulation and prediction including logistic regression, cellular automata, Markov chain, agent-based model and ANN (Parker and Meretsky, 2004; Vázquez-Quintero *et al*., 2016; Wang *et al*., 2018). Cellular automata model has been proved to be very suitable for simulating and predicting complex geographic process (Alexandridis *et al*., 2008; Mitsova *et al*., 2011; Santé *et al*., 2010). The ANN combined with the cellular model can effectively simplify the model structure, which is suitable for simulating complex geographic systems (Qiang and Lam, 2015). In this study, a hybrid model composed of ANN and cellular automata has been used for simulating. At first, the fuzzy module has been employed to standardize the range of LST map into 0 to 1. Next, we reclassified the LST map into ten categories. After this step, each pixel in the LST map has their own precise value to reflect the temperature. Third,

39

the ANN module has been used to calculate the probability of occurrence by employing the LST distribution map in 2015 and modeling variables. Finally, we have used the self-adaptive inertia and competition mechanism CA module to simulate LST in 2025. In this analysis, all the steps have been executed in TerrSet 18.31 and Geo-SOS-FLUS V2.2 software.

3. Results and discussions

3.1. Spatiotemporal changes in Land use/cover and LST

Fig. 3 indicates the normalization result of LST distribution in each land use/cover category with the range between 0 and 1. In 2005, the LST ranged widely because of the high diurnal temperature variation. In contrast, LST's scale was small in 2015 due to the low diurnal temperature variation. Even if there is a difference of diurnal temperature variation between the LST in 2005 and 2015, we could find some similarities. The main LST was increasing from 0.47 in 2005 to 0.51 in 2015, which is consistent with urbanization process in the study area. At the same time, 725.36 km^2 area had been changed from other land use types into the built-up category (Wang and Murayama, 2017). The main LST in cropland increased from 0.38 to 0.44, and high temperature regain changed from the central area to the surrounding area. The main LST in water area also increased from 0.19 to 0.31 without area change. However, the main LST in the green area decreased from 0.47 to 0.38. Conversion from green space to built-up, owing to urbanization, is the main cause of this phenomenon. The LST of each land use/cover category is granted in the lowest to the highest order, based on their location in Tianjin city. The LST in the built-up area is the highest, and the water is the lowest.

3.2. Preparation of modeling variables

For examining the spatial LST pattern, we select DEM, slope, distance to built-up and NDVI as modeling variables. DEM and slope are essential variables of terrain analysis. Different elevation produces different LST, especially in mountain areas. Distance to built-up is generated by using ArcGIS 10.2 software. Built-up expansion is another main source of the LST increase. We also put NDVI as modeling variables because the distribution and density of vegetation are closely related to LST. Finally, we standardize the range into 0 to 255 in all the modeling variables to keep consistency between original dataset.

3.3. Simulation of the LST in 2015 and 2025

Fig. 5 shows the spatiotemporal pattern of the LST in 2005, 2015 and 2025. The ranges of LST maps were normalized into 0 to 1. In this figure, the red color means the higher temperature, on the contrary, the blue means the lower temperature. By comparing these three LST maps, we found that the high temperature area is gradually increasing from 2005 to 2025. The main cause of this phenomenon is the urbanization. When the built-up area is expanding, some cropland and green space are forced to change. Most of water areas are reservoirs except for Binhai port. The LST in water areas is incomparable in three phases because the water storage capacity of reservoirs varies slightly between years and seasons. Fig. 6 shows the probability distribution of the LST in 2005, 2015 and 2025. The highest temperature was in the range of 0.4 to 0.5 in 2005, and 0.6 to 0.7 in 2015. But in 2025, the highest temperature increased to the range of 0.7 to 0.8.

For the modeling validation, we used the LST map and modeling variables in 2005 to simulate the LST in 2015. By comparing the simulation map and actual map in 2015, we found that the total kappa value is 62.17% which can be acceptable in the analysis (van Vliet *et al*., 2011). We found that from 2005 to 2025, the average temperature is increasing progressively. The result is an alert to government and city planners that protecting the environment and the rational assignment of land use/cover are very crucial for sustainable development.

4. Conclusion

The simulation result of LST shows that the temperature increase and the built-up expansion are correlated with each other. The temperature of the cropland surrounded by built-up will continue to increase. Therefore, green space distribution is very crucial to decrease the LST in the future. This result can also help to understand the structure of land use/cover in Tianjin city. Urban planners and the related department of the government should pay more attention to sustainable development and environmental protection. Economic growth and urban development should not be achieved at the expense of long-term environmental damage especially in developing countries.

	Built-up	Cropland	Green area	Water

LST in 2005

Low: 0.08　High: 0.90　Low: 0.01　High: 0.81　Low: 0.10　High: 0.78　Low: 0.01　High: 0.64

Land use/cover distribution in 2005

Built-up　Cropland　Green area　Water

LST in 2015

Low: 0.46　High: 0.54　Low: 0.38　High: 0.49　Low: 0.31　High: 0.48　Low: 0.26　High: 0.38

Land use/cover distribution in 2015

Built-up　Cropland　Green area　Water
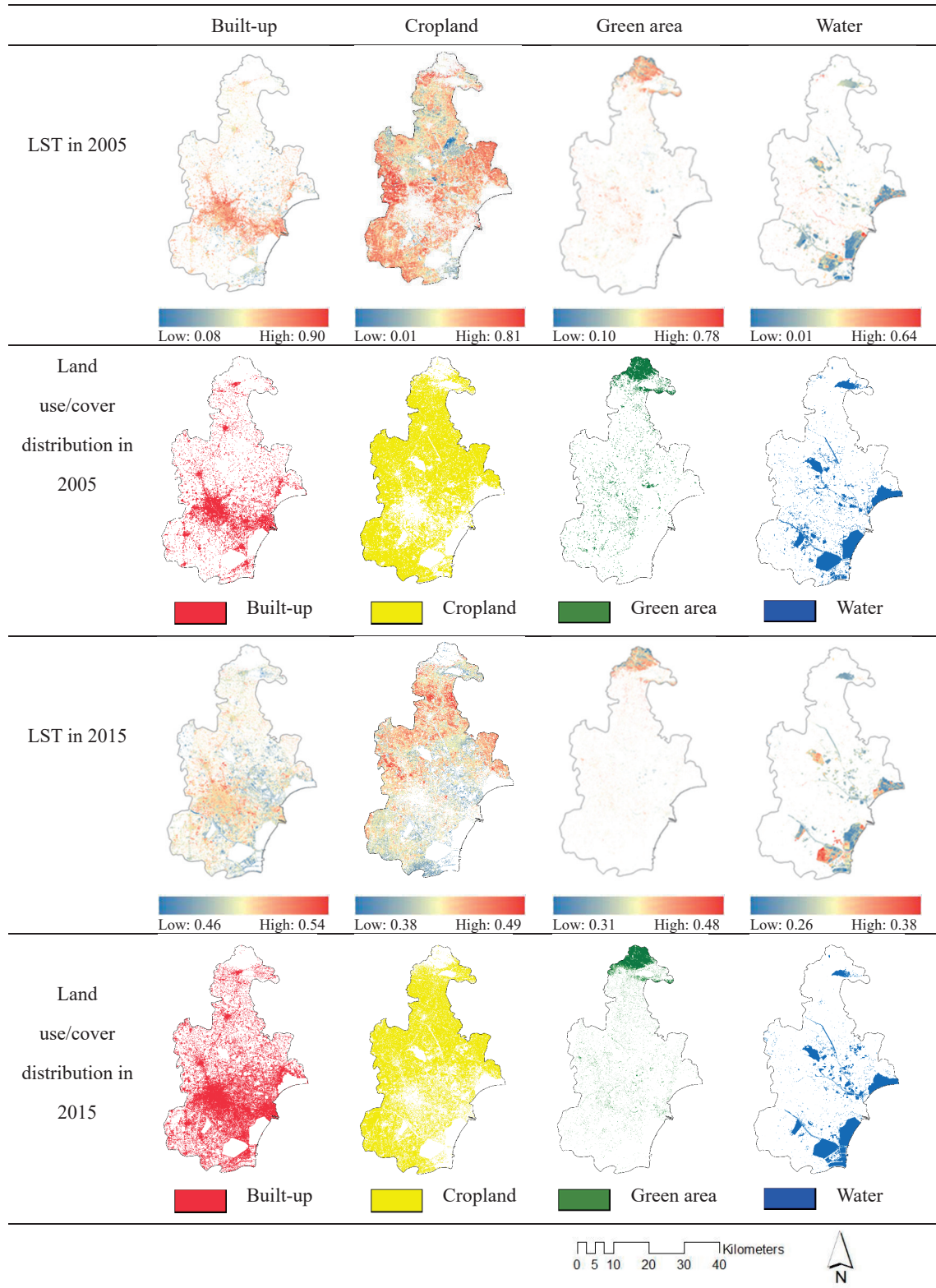
Kilometers
0 5 10 20 30 40　N

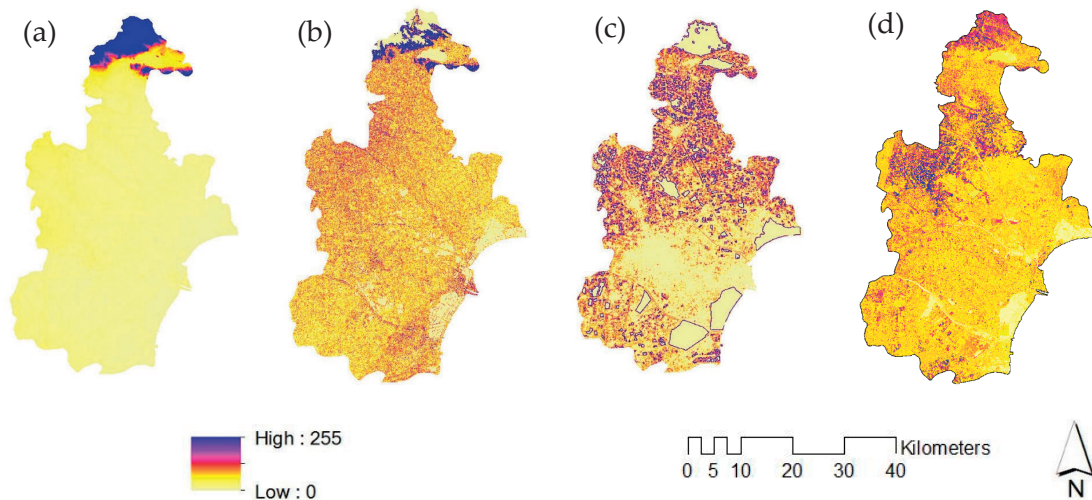Fig. 3. Normalized LST and land use/cover distribution in 2005 and 2015.

Fig. 4. Modeling variables in 2015 in the simulation. (a) DEM; (b) Slope; (c) Distance to built-up; and (d) NDVI.
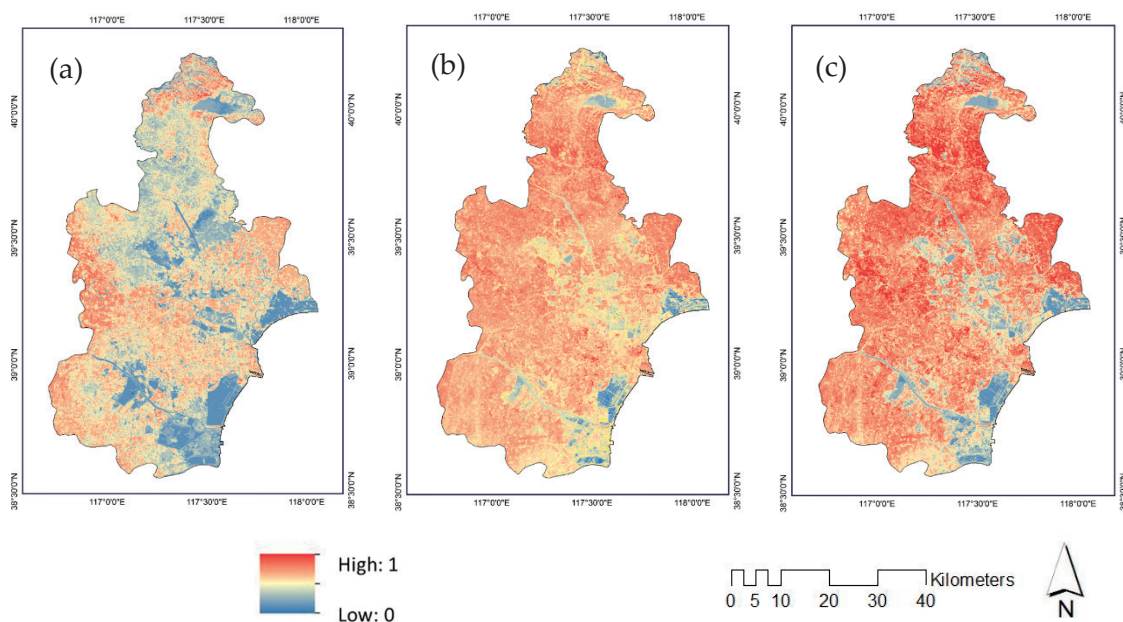

Fig. 5. Normalized LST maps in (a) 2005, (b) 2015, and (c) 2025 (simulated).

References:

Alexandridis, A., Vakalis, D., Siettos, C.I. and Bafas, G.V. (2008): A cellular automata model for forest fire spread prediction: The case of the wildfire that swept through Spetses Island in 1990. *Appl. Math. Comput.*, **204**, 191–201. doi: 10.1016/j.amc.2008.06.046

Estoque, R.C. and Murayama, Y. (2017): Monitoring surface urban heat island formation in a tropical mountain city using Landsat data (1987–2015). IS-PRS *J. Photogramm. Remote Sens.*, **133**, 18–29. doi: 10.1016/j.isprsjprs.2017.09.008

Frihy, O.E. (2017): Evaluation of future land-use planning initiatives to shoreline stability of Egypt's northern Nile delta. *Arab. J. Geosci.*, **10**, 109. doi: 10.1007/s12517-017-2893-4

Hao, H., Estoque, R.C. and Murayama, Y. (2016): Spatio-temporal analysis of urban growth in three African capital cities: A grid-cell-based analysis using remote sensing data. *J. Afr. Earth Sci.*, **123**, 381–391. doi: 10.1016/j.jafrearsci.2016.08.014

Li, J., Song, C., Cao, L., Zhu, F., Meng, X. and Wu, J. (2011): Impacts of landscape structure on surface
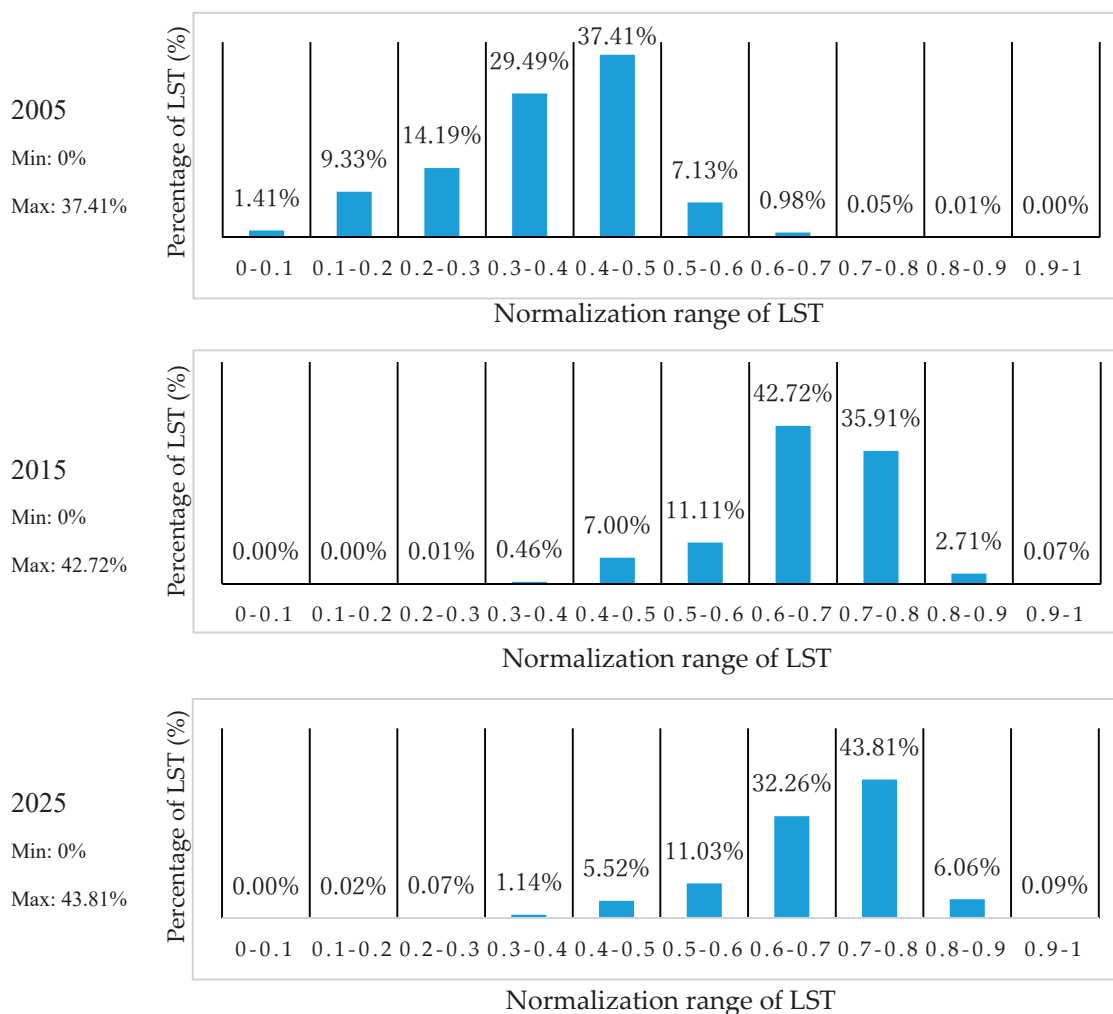
Fig. 6. Probability distribution of the LST in 2005, 2015 and 2025.

urban heat islands: A case study of Shanghai, China. *Remote Sens. Environ.*, **115**, 3249–3263. doi: 10.1016/j.rse.2011.07.008

Li, Z.-L., Tang, B.-H., Wu, H., Ren, H., Yan, G., Wan, Z., Trigo, I.F. and Sobrino, J.A. (2013): Satellite-derived land surface temperature: Current status and perspectives. *Remote Sens. Environ.*, **131**, 14–37. doi: 10.1016/j.rse.2012.12.008

Madurako I., Yun, Z. and Patrick, B. (2016): Simulation and prediction of Land Surface Temperature (LST) dynamics within Ikom City in Nigeria using Artificial Neural Network (ANN). *J. Remote Sens. GIS*, **5**, 1–7. doi: 10.4172/2469-4134.1000158

Mitsova, D., Shuster, W. and Wang, X. (2011): A cellular automata model of land cover change to integrate urban growth with open space conservation. *Landsc. Urban Plan.*, **99**, 141–153. doi: 10.1016/j.landurbplan.2010.10.001

National Bureau of Statistics of China [WWW Document], n.d. Natl. Data. URL http://data.stats.gov.cn/english/ (accessed 5.23.15).

Parker, D.C. and Meretsky, V. (2004): Measuring pattern outcomes in an agent-based model of edge-effect externalities using spatial metrics. *Agric. Ecosyst. Environ.*, **101**, 233–250. doi: 10.1016/j.agee.2003.09.007

Phan, T.N., Kappas, M. and Tran, T.P. (2018): Land surface temperature variation due to changes in elevation in Northwest Vietnam. *Climate*, **6**, 28. doi: 10.3390/cli6020028

Qiang, Y. and Lam, N.S.N. (2015): Modeling land use and land cover changes in a vulnerable coastal region using artificial neural networks and cellular automata. *Environ. Monit. Assess.*, **187**, 57. doi: 10.1007/s10661-015-4298-8

Ranagalage, M., Estoque, R.C., Handayani, H.H., Zhang, X., Morimoto, T., Tadono, T. and Murayama, Y.

(2018): Relation between urban volume and land surface temperature: A comparative study of planned and traditional cities in Japan. *Sustainability*, **10**, 2366. doi: 10.3390/su10072366

Santé, I., García, A.M., Miranda, D. and Crecente, R. (2010): Cellular automata models for the simulation of real-world urban processes: A review and analysis. *Landsc. Urban Plan.*, **96**, 108–122. doi: 10.1016/j.landurbplan.2010.03.001

Song, L. and van Geenhuizen, M. (2014): Port infrastructure investment and regional economic growth in China: Panel evidence in port regions and provinces. *Transp. Policy*, **36**, 173–183. doi: 10.1016/j.tranpol.2014.08.003

Subasinghe, S., Estoque, R.C. and Murayama, Y. (2016): Spatiotemporal analysis of urban growth using GIS and remote sensing: A case study of the Colombo metropolitan area, Sri Lanka. *ISPRS Int. J. Geo-Inf.*, **5**, 197. doi: 10.3390/ijgi5110197

van Vliet, J., Bregt, A.K. and Hagen-Zanker, A. (2011): Revisiting Kappa to account for change in the accuracy assessment of land-use change models. *Ecol. Model.*, **222**, 1367–1375. doi: 10.1016/j.ecolmodel.2011.01.017

Vázquez-Quintero, G., Solís-Moreno, R., Pompa-García, M., Villarreal-Guerrero, F., Pinedo-Alvarez, C. and Pinedo-Alvarez, A. (2016): Detection and projection of forest changes by using the markov chain model and cellular automata. *Sustainability*, **8**, 236. doi: 10.3390/su8030236

Wang, R., Derdouri, A. and Murayama, Y. (2018): Spatio-temporal simulation of future land use/cover change scenarios in the Tokyo metropolitan area. *Sustainability*, **10**, 2056. doi: 10.3390/su10062056

Wang, R. and Murayama, Y. (2017): Change of land use/cover in Tianjin city based on the markov and cellular automata models. *ISPRS Int. J. Geo-Inf.*, **6**, 150. doi: 10.3390/ijgi6050150

Weng, Q., Lu, D. and Schubring, J. (2004): Estimation of land surface temperature–vegetation abundance relationship for urban heat island studies. *Remote Sens. Environ.*, **89**, 467–483. doi: 10.1016/j.rse.2003.11.005

Xu, Y., Qin, Z. and Wan, H. (2010): Spatial and temporal dynamics of urban heat island and their relationship with land cover changes in urbanization process: a case study in Suzhou, China. *J. Indian Soc. Remote Sens.*, **38**, 654–663. doi: 10.1007/s12524-011-0073-7

Zhang, G., Yu, Q., Li, M., Huang, Y., Yue, P. and Wang, J. (2017): Simulation of land surface temperature in Haidian district based on EnKF-3DVar model. *Trans. Chin. Soc. Agric. Mach.*, **48**, 166–172. doi: 10.6041/j.issn.1000-1298 .2017.09.021